Journal of Engineering and Applied Sciences
MEDWELL PUBLICATIONS

Simulation the Effect of Vibroacoustic on Space Vehicle Structures

Mahmoud Fadhel Edan
Department of Civil Engineering, Al-Maarif University College, Ramadi, Iraq

Key words: Space, vehicle, base, acoustic, excitation, simulation

Corresponding Author:
Mahmoud Fadhel Edan
Department of Civil Engineering, Al-Maarif University College, Ramadi, Iraq

Page No.: 1962-1971
Volume: 15, Issue 8, 2020
ISSN: 1816-949X
Journal of Engineering and Applied Sciences

Abstract: In this research, the MATLAB Software was used to simulate the effect of vibroacoustic excitation on space vehicle structures that were able to be represented by using lumped-parameter representation is studied. A ceramic tile which had been created as a portion of the warm assurance framework of the space carry was utilized. These tiles were exclusively joined to the boards of the orbiter through an adaptable cushion. Predicated form direct irregular vibration modules were defined to foresee tile vibrations and energetic stresses due to the broadband acoustic field on the external surface and the base excitation on the reinforced surface. The analytic models were utilized to anticipate vibrations and energetic stresses on chosen tiles. The same representation was used to predict vibrations and dynamic stresses of a payload mass. Finally, conditions were established as to the accuracy of the predicted-form technique.

INTRODUCTION

Typical complex space-vehicle structures usually consist of different types of substructures which make a distributed parameter analysis difficult and often impossible to formulate. Thus, a lumped-parameter representation is one of usually preferred for molding the structure sees reference (Cockburn and Robertson, 1974). Lumped-parameter analysis with random vibration theory are used to explain the vibroacoustic environment of one of the major engineering innovation associated with spacecraft or even with space-shuttle design program under both base excitation (resulted from acoustic excitation) and also direct acoustic excitation. This incorporates establishment of sintered silicate fiber tiles adapt ably joined to the orbiter's aluminum skin (Fig. 1). Each tile is bounded to an orbiter board through a strain separation cushion (Fig. 2). The SIP is a Nomex felt fabric comprising of two layers of joined filaments sewed together. The thickness of the taste is regularly 4.1 mm

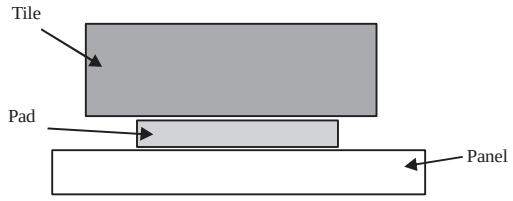

Fig. 1: Tile/pad/panel profile

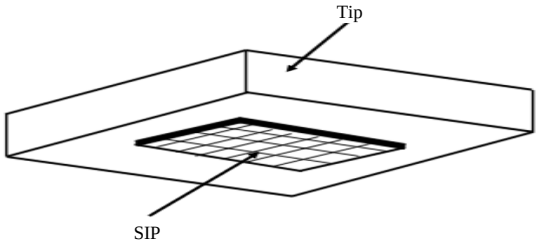

Fig. 2: Tile/pad contact area

the tiles of which there are >30000 (Doyle Jr., 1982) are designed to be a thermal barrier to protect the outer aluminum surface panels of the orbiter from the high temperatures during reentry.

The tiles must be designed for two structurally critical mission phases. These phases are at lift-off and during passage through the tall energetic weight locale of climb. At these times, the vehicle is uncovered to high-level broadband arbitrary weight vacillations that cause the orbiters external boards to vibrate. These irregular vibrations deliver a base excitation stack on the tile. The real dynamic reaction may be a coupled movement between the tiles and boards with the acoustic field acting as the constraining work. A linear analytical model is used to predict tile vibrations as so as loads at the tile/SIP interface. Also, the study is extended to include six different positions of tiles in a space-shuttle to show the most worried region that suffering from acoustic excitation. The equations of this model were used to estimate the vibrations of large masses such as payload mass by substituting tile's mass by the later mass and using adopted values of dynamic characteristics of natural frequency with different values of damping ratio to explain the behaviour of different damping materials. The acoustic levels are chosen of four different spacecraft measured experimentally (Bernet, 1989) in addition, typical base excitation is used to estimate payload vibration under such excitation (Osgood, 1966).

Mission environment: The acoustic fields surrounding the orbiter during lift off and ascent have been established according to reference (Cockburn and Robertson, 1974) where these areas have been built up by small-scale tests and by comparison with full-scale saturn V lift-off. The weight were decided at particular areas and after that generalized to locales of the orbiter's external boundaries. The acoustic field for each locale was arranged as a sound pressure level for one-third octave groups from 20-2000 Hz. Figure 3 appears the most extreme acoustic weight at lift off for the body fold of six tiles in a space carry in Fig. 4. The acoustic field of these tiles were specified in Power Spectral Density from (PSD). The orbiter panel vibrations were given in terms of acceleration Power Spectral Density (PSD)(Cockburn and Robertson, 1974) (Fig. 5). The acceleration PSD's were generally specified from 20-2000 Hz. Generally, the acceleration PSD specifications were characterized by a constant value over several hundred hertz and a three, six or nine dB/octave roll off on either side of the constant level.

Both PSD's shown in Fig. 4 and 5 are envelopes of many test results. They, therefore, represent conservative estimates of the total random environment that would be experienced by a tile. They do not include the effect of shocks.

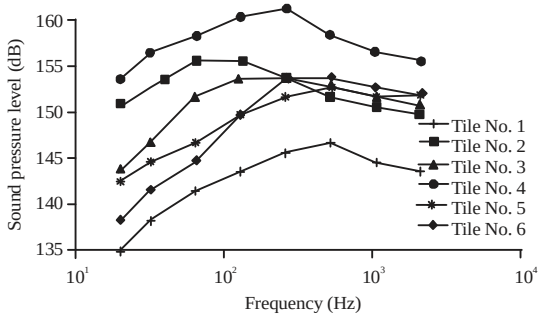

Fig. 3: Sound pressure level of six orbiters at different positions in a space shuttle

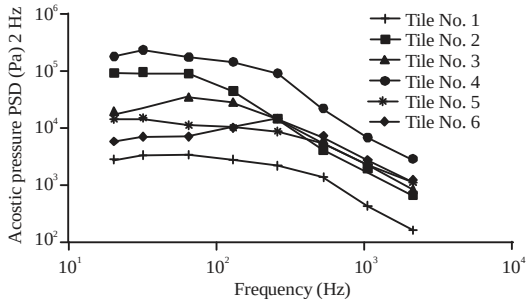

Fig. 4: Acoustic pressure of six orbiters at different positions in a space shuttle

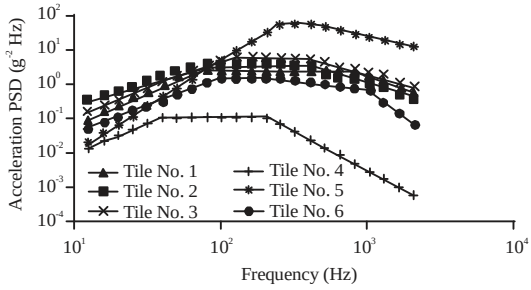

Fig. 5: Vibrations of six orbiters at different positions in a space shuttle (Typical base excitation level of a spacecraft)

Mathematical models assumptions: To create a sensibly basic strategy of examination for the tile's irregular vibrations, it was fundamental to consider a number of simplifying assumption. The legitimacy of the examination coming about from these suspicions can be illustrated by more detailed examination procedures or in a perfect world by testing. Each tile is considered as an autonomous component subjected to the arbitrary vibrations of an orbiter surface board and the weight vacillations of the acoustic field, the two wonders have been analyzed independently and combined to allow a add up to vibroacoustic stacking. Since, both driving capacities are wide-band excitation in recurrence space,

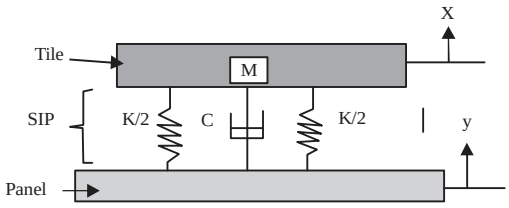

Fig. 6: Base excitation of a linear mass/spring/damper system

an irregular vibration approach is vital to foresee both vibrations and stacking. In so doing, a cruel square reaction is decided and after that changed over to a three-sigma stacking, based on the conservative input excitations (Fig. 4 and 5), a three-sigma design load is a reasonable upper bound for design and was so, specified for the space shuttle by NASA. The three-sigma level would not incorporate disastrous occasions such as stuns. Within the investigation of the tile reaction, the takings after extra assumptions are made:

The tile may be a rectangular, symmetric, inflexible mass vibrating opposite to the board only. The SIP is modelled with proportionate direct solidness and damping components, to be decided from arbitrary tests. The base excitation and acoustic weight PSD's are at first spoken to as a steady esteem over frequencies from zero to an esteem much more prominent than the common recurrence of the tile on the SI.

Base excitation: For a single degree of freedom system linear model (Fig. 6), the relationship between input excitation and output response is given as (Osgood, 1966):

$$S_{\ddot{x}}(\omega) = |H(\omega)|^2 S_{\ddot{y}}(\omega) \quad (1)$$

Equation 1 is used to estimate tile vibrations as acceleration PSD where is the panel acceleration as shown by Fig. 5. Now, the mean square acceleration response of the tile is:

$$[\ddot{X}^2] = \int_{-\infty}^{\infty} S_{\ddot{x}}(\omega)d\omega \quad (2)$$

By substituting of Eq. 1 into Eq. 2 yields:

$$[\ddot{X}^2] = \int_{-\infty}^{\infty} |H(\omega)|^2 S_{\ddot{y}}(\omega)(\omega)d\omega \quad (3)$$

The transfer function squared for a linear, single degree of freedom, base excited system (Fig. 6) is given as:

$$|H(\omega)|^2 = |H(f_i)|^2 = \frac{1+(2\xi r)^2}{(1-r^2)^2+(2\xi r)^2}$$

With the assumption that the panel acceleration PSD is constant over all frequencies and also by substitution of linear transfer function, the mean square acceleration of Eq. 3 is given by Newland (1975):

$$[\ddot{X}^2] = \frac{S_{\ddot{y}}\pi f_n(4\xi^2+1)}{4\xi} \quad (4)$$

The plan push within the SIP (or at the tile/SIP interface) is given as the three-sigma esteem (Cockburn and Robertson, 1974). In case the cruel esteem of push is zero, the three-sigma stretch esteem is:

$$P_d = \frac{3W[\ddot{X}^2]^{1/2}}{A_s} \quad (5)$$

Finally, substituting Eq. 4 into Eq. 5 yields:

$$P_d = \frac{3W}{A_s}\left[\frac{\bar{S}_{\ddot{y}}\pi f_n(4\xi^2+1)}{4\xi}\right]^{1/2} \quad (6)$$

Equation 6 could be a predicated form expression for the plan load within the SIP due to a broadband, arbitrary, base excitation. Among other limitation, it was expected that the board increasing speed PSD was steady. From a commonsense SIP, Condition 5 will predict excessively preservation esteem for the load. As appeared afterward within order of words about, the common frequency of the tile was as a rule within the frequency extends of the consistent esteem board speeding up PSD. In this manner Equation 6 give a basic, traditionalist expression for base excitation load. When the consistent esteem panel increasing speed PSD presumption was loose, a numerical arrangement is received utilizing the essential expression given in Eq. 1 and 2. An expression identical to Eq. 4 is:

$$[\ddot{x}^2] = \sum_{i=1}^{N} |H(f_i)|^2 S_{\ddot{y}}(f_i)\Delta f_i \quad (7)$$

Where, is the band width of ith one-third octave band channel and f is the center frequency of each band. In Eq. 7, both the exchange work and the panel speeding up PSD are to be assessed at the center frequency of each one-third octave band. The three-sigma load for numerical arrangement is given by substituting Eq. 7 into Eq. 5. Whether Eq. 4 or 7 is utilized to decide the mean square speeding up of the tile on the SIP, it is obvious that the energetic characteristics of the tile/SIP framework must be known. In Eq. 4, the tile/SIP normal frequency and damping proportion must be known. Moreover in Eq. 7 the tile board exchange work must be known for all frequency groups of intrigued. For a straight single degree

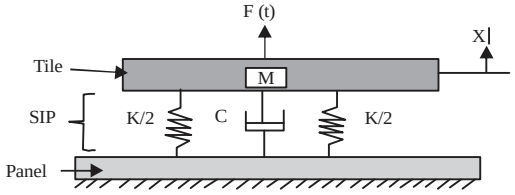

Fig. 7: Constrained excitation of a direct mass-spring-damper system

of flexibility oscillator information of the characteristic frequency and damping proportion gives a direct exchange work. In any case, in the event that the exchange work may be a nonlinear work of excitation (Eq. 7) can still be utilized to anticipate the response. That nonlinear exchange work would get to be decided by arbitrary tests beneath practical loading. Since, the SIP fabric was not recently created but point by point energetic characteristics were not accessible at the time of this advancement. Hence, a straight exchange work with equivalent solidness and damping is utilized in predicating the tile vibrations and loads that are given within the results.

Acoustic excitation: Both tile vibration and dynamic load within the SIP due to the acoustic field (Fig. 4) is to be decided in a way comparative to that determined for the base excitation case. The relationship between the acoustic weight PSD and the tile relocation PSD for a constrained, one degree-of-freedom framework (Fig. 7) is given by Osgood (1966). Equation 8 is utilized to assess tile displacement PSD under coordinate acoustic excitation. The mean square relocation of the tile is now,

$$[X^2] = \int_{-\infty}^{+\infty} S_x(\omega)d\omega \tag{9}$$

The transfer function squared of Eq. 8 is:

$$|H_1(\omega)|^2 = |H(f_i)|^2 = \frac{(A_t/K)^2}{(1-r^2)^2+(2\xi r)^2}$$

With the assumption that acoustic pressure PSD is constant over all frequencies, the mean square displacement of the tile using Eq. 9 is:

$$[X^2] = \int_{-\infty}^{+\infty} |H_1(\omega)|^2 S_p(\omega)d\omega \tag{10}$$

Substituting of in Eq. 10 and using residue theorem to evaluate the above integral yield:

$$[X^2] = \frac{S_p A_t^2}{64\pi^3\xi M^2 f_n^3} \tag{11}$$

In the same manner, the relationship between the acoustic pressure PSD and tile velocity PSD is given as:

$$S_{\ddot{x}}(\omega) = |H_2(\omega)|^2 S_p(\omega) \tag{12}$$

where, Eq. 1 used to estimate tile velocity, if it is necessary. The transfer function squared is:

$$|H_2(\omega)|^2 = |H_2(f_i)|^2 = \frac{(2\pi f_i A_t/K)^2}{(1-r^2)^2+(2\xi r)^2}$$

And the mean square velocity response is:

$$[\ddot{X}^2] = \int_{-\infty}^{+\infty} S_{\ddot{x}}(\omega)d\omega \tag{13}$$

With the presumption that the acoustic pressure PSD is steady over all frequencies and by substitution of Eq. 12 into Eq. 13 abdicate:

$$[\ddot{X}^2] = \int_{-\infty}^{+\infty} |H_2(\omega)|^2 S_p(\omega)d\omega \tag{14}$$

Substitution of $|H_2(\omega)|^2$ and evaluating integral of Eq. 14 yield:

$$[\ddot{X}^2] = \frac{\overline{S_p}\hat{A}_t^2}{16\pi\xi M^2 f_n} \tag{15}$$

The three sigma stretch within the SIP due to the compelling damping and solidness components of the material are:

$$P_k = \frac{3K}{A_s}[X^2]^{1/2} \tag{16}$$

$$P_a = \frac{3C}{A_s}[\ddot{X}^2]^{1/2} \tag{17}$$

Since, for harmonic movement, damping and solidness powers are out of phase, the entire compelling push within the SIP due to the acoustic field is given by:

$$P_a = [P_k^2 + P_a^2]^{1/2} \tag{18}$$

Combining Eq. 11, 15, 16 and 17 yields:

$$P_a = \frac{3A_t}{A_s}\left[\frac{\bar{S}_p \pi f_n (4\xi^2+1)}{4\xi}\right]^{1/2} \quad (19)$$

As with base excitation, it is accepted at first that the PSD of the acoustic pressure is consistent for all frequencies. Just like the base excitation PSD, the acoustic weight PSD may shift by more than an arrange of size altogether below the common frequency of the tile. Hence, utilizing the acoustic pressure PSD at the characteristic frequency in Eq. 19 may significantly under assess the stretch within the SIP. A comparable explanation around the expression for base of frequencies closes the tile common recurrence. Discrediting Eq. 8 and 9, an expression for the mean square displacement of the tile is given by:

$$[X^2] = \sum_{i=1}^{N} |H_1(f_i) \quad (20)$$

And:

$$[\ddot{X}^2] = \sum_{i=1}^{N} |H_2(f_i) \quad (21)$$

Where, $S_p(f_i)$ is given by:

$$S_p(f_i) = \frac{1}{\Delta f_i}[2\times10^{-5}\times10^{(dB/20)}]^2 \frac{(Pa)^2}{Hz} \quad (22)$$

Substituting of Eq. 20 and 21 into Eq. 16 and 17 and after that into Eq. 18, gives a more precise esteem than Eq. 19 for the dynamic stress within the SIP due to acoustic field.

Now, the acceleration PSD of the tile (mass) under the effect of acoustic pressure PSD ($S_p(\omega)$) is to be estimated. The relationship used for this purpose which connect between tile acceleration PSD and acoustic pressure PSD is:

$$S_{\ddot{x}}(\omega) = |H_3(\omega)|^2 S_p(\omega) \quad (23)$$

Where, $|H_3(\omega)|^2$ is:

$$|H_3(\omega)|^2 = \frac{(r^2 A_t/M)^2}{(1-r^2)^2+(2\xi r)^2}$$

Total three-sigma load: The two dynamic loads given by Eq. 6 and 19 are two unmistakable arbitrary loading phenomena but they are not free. It is in this manner expected that the staging between the stresses changes haphazardly which the overall three sigma stress can be communicated as:

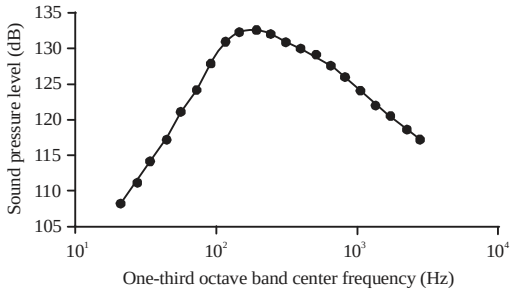

Fig. 8: Sound pressure level of the acoustic

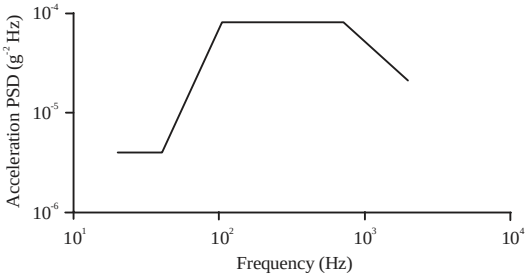

Fig. 9: Typical base excitation level of spacecraft

$$P_t = \left[P_a^2 + P_d^2\right]^{1/2} = \frac{3}{A_s}\left[\pi f_n\left(\frac{4\xi^2+1}{4\xi}\right)\left(\bar{S}_p A_t^2 + \bar{S}_{\ddot{y}} W^2\right)\right]^{1/2} \quad (24)$$

Generalizing of the mathematical model: All the above derived equations for both types of excitation is true to application to systems that are able to be simulated by lumped parameter representation whether large masses are used or not, all that needed is the dynamic characteristics of the vibrating system into the excitation field to estimate system vibrations. On this basis a whole payload mass of 200 kg with surface area (1 m^2) is used as the lumped mass to estimate it's vibration under four deferent levels of acoustic pressure of space craft's (Arian) Fig. 8 (Doyle Jr., 1982) with typical base excitation of spacecraft (Fig. 9), (Bernet, 1989), used to base excitation. A natural frequency value (50 Hz) is used as the natural frequency of the payload mass according to the recommended range of the natural frequency of a spacecraft of 50-120 Hz (Bernet, 1989). Using the above levels of acoustic pressure and base excitation with the assumed natural frequency value and different values of damping ratio, the vibration of the payload mass were estimated.

Predictive results for selected tiles

Tile specification: To predict both vibration and loads (stresses) of space-vehicle orbiter TPS, six models are used.

Table 1: Vibroacoustic analysis parameters

Tile/Orbiter location	Tile natural frequency (Hz)	SIP area (cm^2)	Tile area (cm^2)	Tile weight (kg)
1/Upper wing near tip	380	135.5	206.50	0.0680
2/Rear of front structure	250	64.5	116.13	0.0726
3/Base heat shield	280	64.5	116.13	0.0590
4/Front of front structure	230	113.5	175.50	0.2860
5/Top of vertical fin	380	58.0	103.20	0.0286
6/Center rear body flap	200	161.3	232.30	0.2860

Excitation of ARIAN spacecraft: Two of them to predict tile's vibrations as PSD and the other four models are to predict tile/SIP stresses utilizing both predicted. To supply an agent behavior of tile vibrations and tile/SIP loading due to the vibroacoustic environment, six orbiters tiles are chosen to consider their behavior, for each chosen tile, drawings were obtained to decide the precise geometry and weight of the tile and taste and its area on the orbiter. The TPS properties, the acoustic field and panel vibration determinations for all specified models are utilized to predict vibrations and loads beneath both base and acoustic excitation. To completely get it the vibroacoustic environment to which the tiles are uncovered, the acoustic pressure and acceleration PSD's for six locales of the orbiter are outlined in Fig. 4 and 5. These districts demonstrate the foremost extreme areas on the orbiter. Figure 5 appears that the common frequency of each tile happens at or close the most extreme acceleration PSD frequency extend of the specific board to which it is connected. On the other hand, the greatest esteem of acoustic pressure PSD is ordinarily much more prominent than the acoustic pressure PSD at the normal frequency of the tile as appeared in Fig. 4. Tile (6) appears distinctive behavior, where the self-evident suggestion of this event is that, since the exchange work is close 1.0 for the energizing recurrence essentially amplify the greatest values of the input acoustic driving. The characteristic recurrence of each tile was scaled depending on a full scale acoustic testing carried out at JSC at NASA (Cockburn and Robertson, 1974). The scaling included the impact of tile weight, the SIP region and its thickness. Different damping ratios are used to examine the behavior of SIP material and other materials in case of selected as a damping material. Since, the SIP is smaller in size than the tile, its area determined by subtracting 13 mm (0.5 in) from each edge of the tile inner surface. Table 1, gives tile/SIP parameters and orbiter (panel) locations for each of the six tile which are studied.

Base excitation effect: Figure 10-15 show the vibrations of the six tiles under the effect of base excitation. Each figure can be divided into three ranges of frequencies, low, medium, high ranges. For tile No. 1 the low frequency range 20-200 Hz shows that the output tile acceleration PSD is identical to that of the input panel

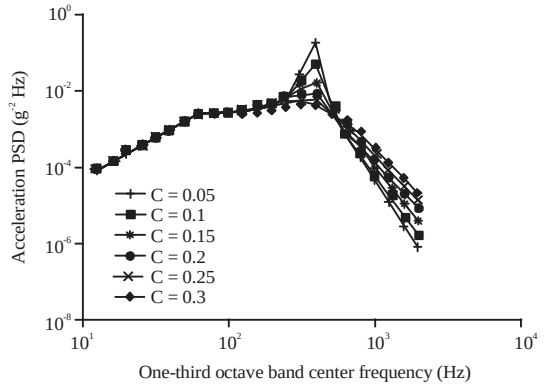

Fig. 10: Acceleration response of tile No. 1 of base-excited system

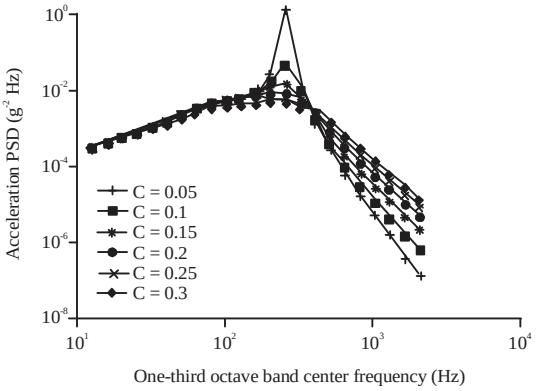

Fig. 11: Acceleration response of tile No. 2 of base-excited system

acceleration PSD. This provides that the variation of damping has no effect in this range of frequency because the transfer function is nearly equal to 1.0. Therefore, no amplification or attenuation will occur to the output tile response. This indicates that whether the damping material is exist or not, no difference in output response will occur. The other tiles behave exactly as tile No. 1 in the low frequency range. In the medium frequency range (200-500 Hz), the acceleration of tile No. 1 is increased until it reaches the maximum value when the exciting frequency coincides with the tile natural frequency. Also, the transfer function is participate in maximizing the tile

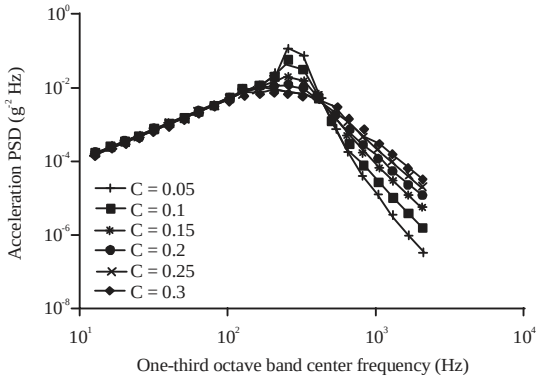

Fig. 12: Acceleration response of tile No. 3 of base-excited system

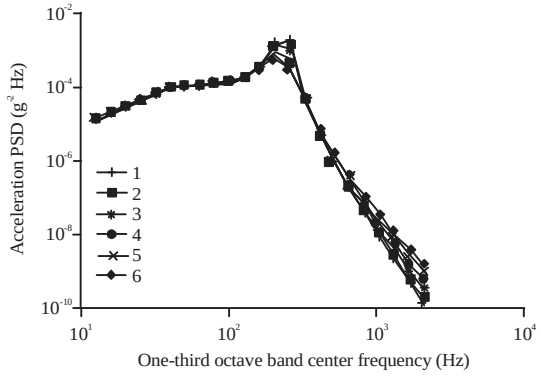

Fig. 13: Acceleration response of tile No. 4 of base-excited system

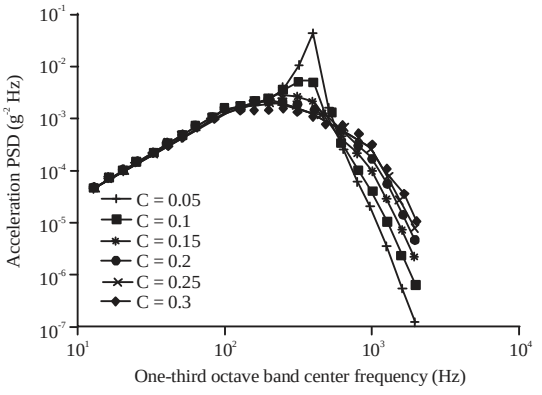

Fig. 14: Acceleration response of tile No. 5 of base-excited system

vibrations where it's value become larger than 1.0. After natural frequency the tile vibration tends to reduce because the value of the transfer function becomes <1.0. The damping variation has an important effect as shown in figures in which the vibrations decreased as well as the

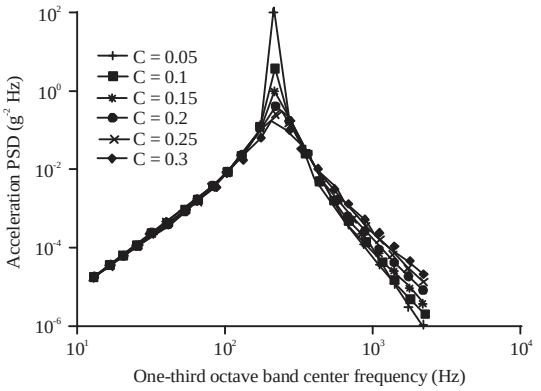

Fig. 15: Acceleration response of tile No. 6 of base-excited system

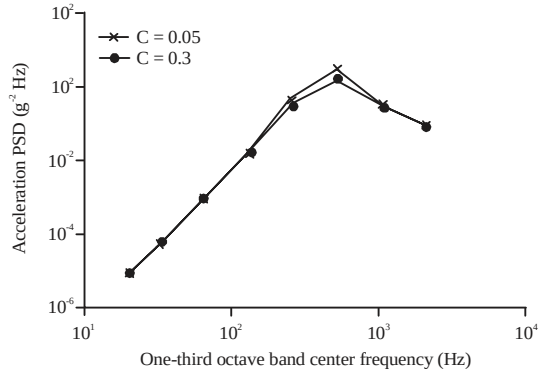

Fig. 16: Acceleration response of tile No. 1 of acoustic-excited system

damping is increased. An inflection point is shown at 500 Hz where all vibrations take the same value because the transfer function takes a constant value at this frequency. After this point the high frequency range (500-2000 Hz) shows an inverse behavior to that of medium frequency range. The output tile acceleration PSD is decreased much greater in small damping ratios than that of large damping ratios because:

- The panel acceleration PSD is also decreasing
- The transfer function is <1.0
- The transfer function value at small damping ratios is smaller than that at larger values of damping ratios which explain the inverse behavior of this region

Direct acoustic excitation effect: Figure 16-21 show the acceleration PSD of six tiles under the effect of direct acoustic excitation. As in base excitation, each figure can be divided into three main ranges of frequency. Figure 16 shows that the damping variation for tile No. 1 has no effect in the low frequency range (20-160 Hz), since, the term in the transfer function of Eq. 23 has insignificant effect to make real variation in response and therefore, the

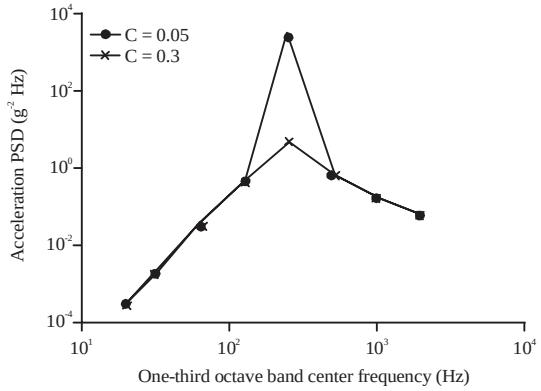

Fig. 17: Acceleration response of tile No. 2 of acoustic-excited system

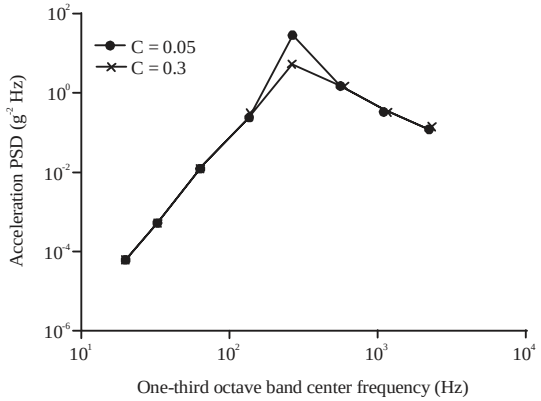

Fig. 18: Acceleration response of tile No. 3 of acoustic-excited system

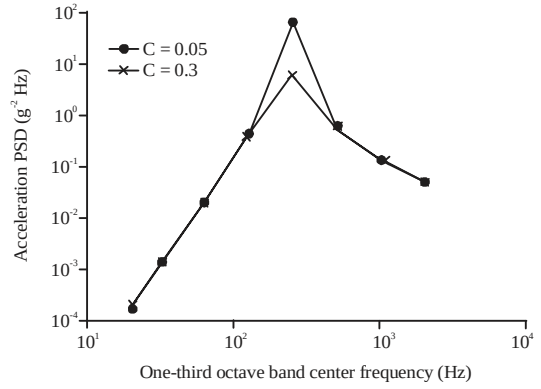

Fig. 19: Acceleration response of tile No. 4 of acoustic-excited system

transfer function will have a value <1.0 in order to minimize the effect of acoustic pressure PSD for this range of frequency. In the medium frequency range (160500 Hz) the damping variation has clear effect to increase the output response specially at tile natural

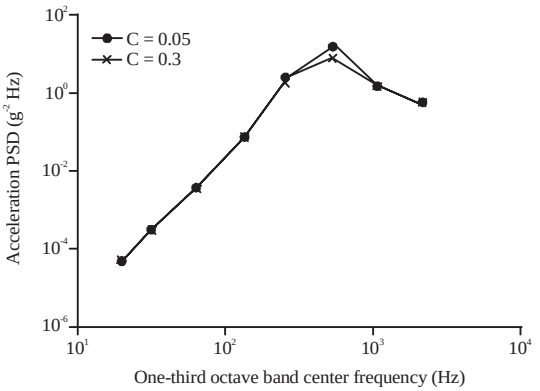

Fig. 20: Acceleration response of tile No. 5 of acoustic-excited system

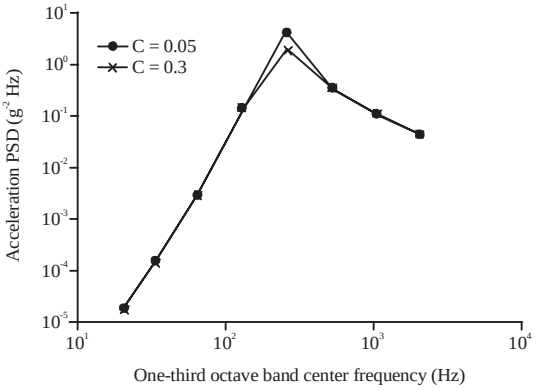

Fig. 21: Acceleration response of tile No. 6 of acoustic-excited system

frequency because of: the exciting frequency coincides with tile natural frequency and the resonance is achieved. The transfer function value participates in maximizing the output acceleration PSD. After the natural frequency the tile vibrations decrease, since, the transfer function becomes <1.0 until it reach a point where all responses take the same path. In the high frequency range (500-2000 Hz) the tile will give the same behavior under different values of damping ratio, therefore, the selection of high damping material will assist in putting down the vibrations at the medium region of frequencies. The main reasons that make tile acceleration PSD decreasing in high frequency range are:

- The acoustic pressure PSD is also decreasing in this range of frequencies
- The transfer function has a value <1.0 as shown in figures the other tiles behave like tile No. 1 and therefore, the same discussion is also true for them

Tile/SIP stresses (base and acoustic excitation): For base and acoustic excited loads (stresses), the predicted

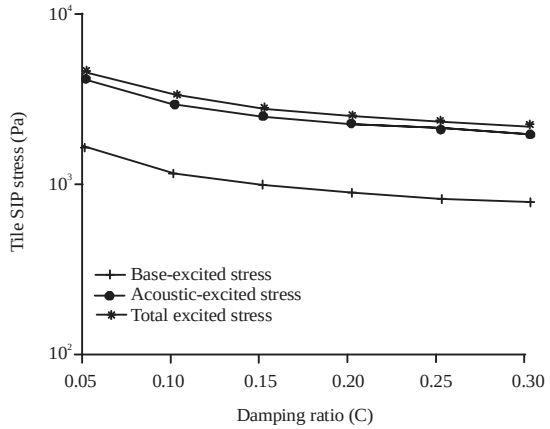

Fig. 22: Predication of three-sigma base, acoustic and total excited stresses in tile/SIP of tile No. 1

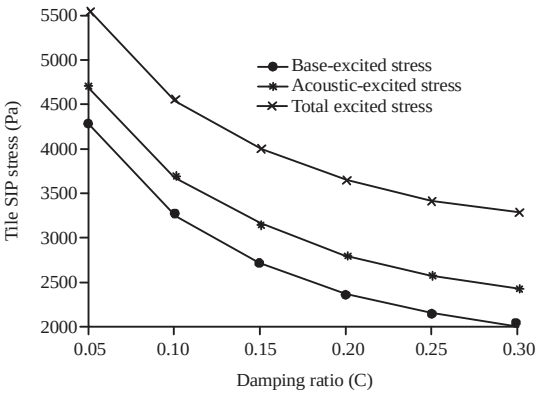

Fig. 23: Predication of three-sigma base, acoustic and total excited stresses in tile/SIP of tile No. 2

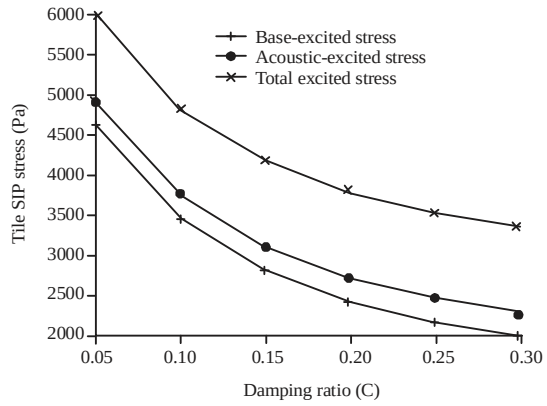

Fig. 24: Predication of three-sigma base, acoustic and total excited Stresses in tile/SIP of tile No. 3

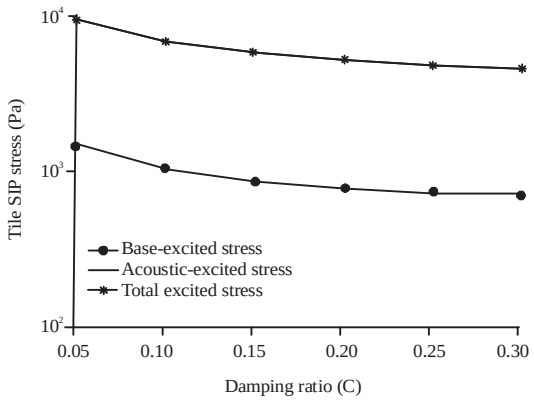

Fig. 25: Predication of three-sigma base, acoustic and total excited stresses in tile/SIP of tile No. 4

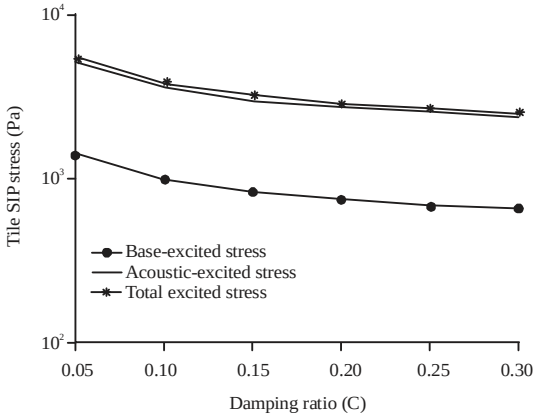

Fig. 26: Predication of three-sigma base, acoustic and total excited stresses in tile/SIP of tile No. 5

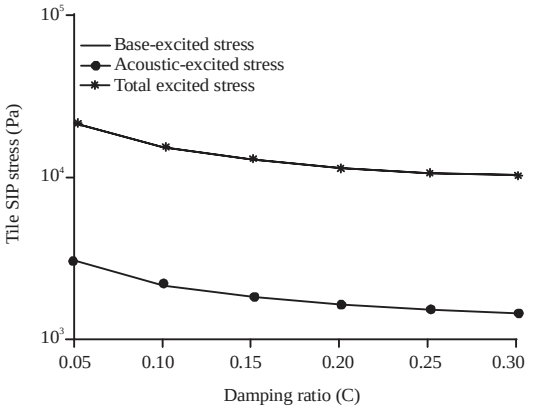

Fig. 27: Predication of three-sigma base, acoustic and total excited Stresses in tile/SIP of tile No. 6

form solution results with their total stress are shown in Fig. 22-27. When the tile natural frequency did not related to the frequencies of maximum panel acceleration (e.g., tiles 4-6) or maximum acoustic pressure (e.g., tiles 1-5), there is a clearly difference between the predicted form solution results as shown in Fig. 23 and 26. We can say that this difference is overly conservative. Since, the tiles most prominent reaction (at their common frequency) was

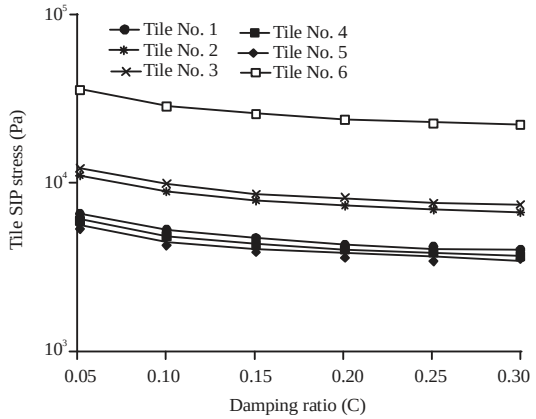

Fig. 28: Total tile/SIP stress versus damping ratio of six tiles under base excitation effect

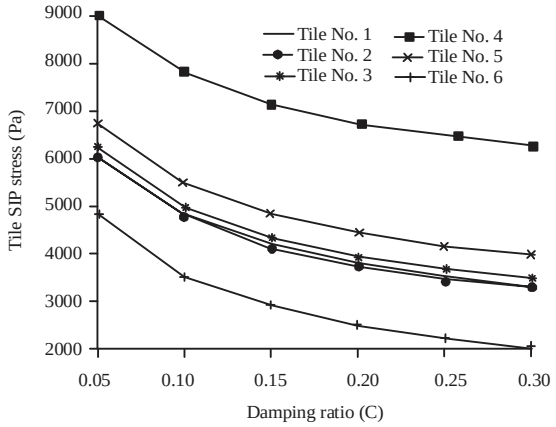

Fig. 29: Total tile/SIP stress versus damping ratio of six tiles under acoustic excitation effect

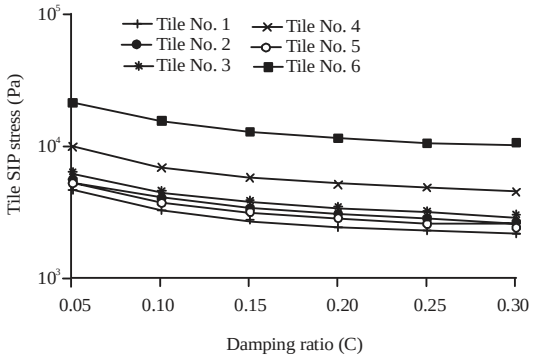

Fig. 30: Total predicted tile/SIP stress versus damping ratio of six tiles under both base and acoustic excitation effect

not at the frequency of most noteworthy panel acceleration or acoustic pressure PSD's. In all the above curves the effect of increasing damping is positively resulted in decreasing the tile/SIP stresses. Total tile/SIP stress versus damping ratio of six tiles under base excitation effect as shown in Fig. 28, under acoustic excitation effect as in Fig. 29. Total predicted tile/SIP stress versus damping ratio of six tiles under both base and acoustic excitation effect as shown in Fig. 30.

CONCLUSION

For base excited system, the damping has no effect in low frequency region (e.g., 20-200 Hz) for tile No. 1) tile vibrations and has a significant effect in medium frequency region (200-500 Hz) where the tile vibration increases reaching the maximum at resonance and then decreases as the damping increases while an inverse behavior is shown in high frequency region (500-2000 Hz). For acoustic excited system, the results show that the damping have no effect in low and high frequency regions while it has a significant effect in medium frequency region.

The predicated form solution are slightly conservative than the numerical solution as the natural frequency of the tile is within the frequency range of maximum PSD level of the forcing function (tiles 1-3) in case of base excitation and tile 6 in case of acoustic excitation). Also, the results are overly conservative when the natural frequency of tile is not within the frequency range of the maximum PSD level of the forcing function (tiles 4-6 in case of base excitation and (tiles 1-5 in case of acoustic excitation). The tile/SIP stresses decreases as the damping ratio increases in both and acoustic excitation. The total tile/SIP stresses results indicates that tile No. 6 is the most severe region and must be designed well.

The base excitation effect resulted from acoustic excitation is more than that of direct acoustic excitation. The using of TPS blanket is so, useful in protecting the space vehicles orbiter from acoustic excitation.

REFERENCES

Bernet, J., 1989. Acoustic effects on spacecraft. Acoust. Bull., 1: 19-23.

Cockburn, J.A. and J.E. Robertson, 1974. Vibration response of spacecraft shrouds toin-flight fluctuating pressures. J. Sound Vibr., 33: 399-425.

Doyle Jr., G.R., 1982. Vibroacoustic modeling for space shuttle orbiter thermal protection system. J. Spacecraft Rockets, 19: 263-268.

Newland, D.E., 1975. An Introduction to Random Vibrations and Spectral Analysis. Longman Publishing Company, Harlow, UK., ISBN: 9780582463349, Pages: 285.

Osgood, C.C., 1966. Spacecraft Structures. Prentice-Hall, Upper Saddle River, New Jersey, USA., Pages: 249.